NG2 cells generate both oligodendrocytes and gray matter astrocytes

Xiaoqin Zhu[1], Dwight E. Bergles[2] and Akiko Nishiyama[1],*

NG2 glia constitute a fourth major glial cell type in the mammalian central nervous system (CNS) that is distinct from other cell types. Although circumstantial evidence suggests that some NG2 glia differentiate into oligodendrocytes, their in vivo fate has not been directly examined. We have used the bacterial artificial chromosome (BAC) modification technique to generate transgenic mice that express DsRed or Cre specifically in NG2-expressing (NG2+) cells. In NG2DsRedBAC transgenic mice, DsRed was expressed specifically in NG2+ cells throughout the postnatal CNS. When the differentiation potential of NG2+ cells in vitro was examined using DsRed+NG2+ cells purified from perinatal transgenic brains, the majority of the cells either remained as NG2+ cells or differentiated into oligodendrocytes. In addition, DsRed+NG2+ cells also differentiated into astrocytes. The in vivo fate of NG2 glia was examined in mice that were double transgenic for NG2creBAC and the Cre reporter Z/EG. In the double transgenic mice, the Cre reporter EGFP was detected in myelinating oligodendrocytes and in a subpopulation of protoplasmic astrocytes in the gray matter of ventrolateral forebrain but not in fibrous astrocytes of white matter. These observations suggest that NG2+ cells are precursors of oligodendrocytes and some protoplasmic astrocytes in gray matter.

KEY WORDS: NG2 (CSPG4), Oligodendrocyte, Progenitor cell, Astrocyte, Myelin, Transgene, FACS

INTRODUCTION

Glial cells in the mammalian central nervous system (CNS) that express the NG2 proteoglycan [also known as chrondroitin sulfate proteoglycan 4 (CSPG4) – Mouse Genome Informatics; NG2 glia] begin to appear during late embryonic stages and rapidly expand to uniformly occupy the entire CNS. These cells are distinct from mature oligodendrocytes, astrocytes or resting ramified microglia and represent a fourth major glial population (Dawson et al., 2000; Dawson et al., 2003; Nishiyama et al., 2002; Peters, 2004). In culture they give rise to oligodendrocytes and are thus called oligodendrocyte precursor cells (OPCs). The term 'OPCs' is used instead of NG2 glia throughout this manuscript to refer to cells that give rise to oligodendrocytes or to cells whose identity had not been confirmed by NG2 immunolabeling.

Direct demonstration of the fate of NG2 glia in vivo has been difficult, as NG2 expression is downregulated before they undergo terminal differentiation. Indirect evidence that NG2 glia differentiate into oligodendrocytes has been obtained from double immunolabeling for NG2 and oligodendrocyte antigens. A small fraction of NG2-expressing cells in normal and demyelinated lesions also express oligodendrocyte antigens (Levine et al., 1993; Nishiyama et al., 1996a; Trapp et al., 1997; Polito and Reynolds, 2005). Demonstration by Reynolds and Hardy (Reynolds and Hardy, 1997) that all NG2-expressing cells in both gray and white matter of the mature rat brain express the immature oligodendrocyte antigen O4 has provided strong support for the notion that NG2 glia are committed precursors of the oligodendrocyte lineage. Additional evidence that NG2 glia give rise to oligodendrocytes was obtained by pulse-chase labeling with 5-bromo-2′-deoxyuridine (BrdU) combined with immunolabeling for cell type-specific antigens at the age and location where the majority of the proliferating cells are NG2 glia. In these areas, which include the juvenile and adult spinal cord, BrdU-incorporated cells were seen to turn into mature oligodendrocytes over time in normal and demyelinated tissues (Bu et al., 2004; Horner et al., 2000; Watanabe et al., 2002; McTigue et al., 2001). It still remains unclear whether these cells go on to become myelinating oligodendrocytes.

The question of whether NG2 glia can give rise to astrocytes has not yet been entirely solved. It is well established that in culture, OPCs can give rise to both oligodendrocytes and type-2 astrocytes (Raff et al., 1983). The search for an astrocytic fate of NG2 glia in vivo has not yielded positive results because of the lack of evidence for the existence of cells that co-express NG2 and astrocytic markers and the lack of evidence that transplanted OPCs generate astrocytes in the CNS (Reynolds et al., 2002; Nishiyama et al., 2002; Nishiyama et al., 2005; Groves et al., 1993; Espinosa de los Monteros et al., 1993). Other studies, however, suggest that there may be glial progenitor cells that can give rise to both oligodendrocytes and astrocytes. Rao and Mayer-Proschel identified glial-restricted precursors that generate astrocytes and oligodendrocytes but not neurons (Rao and Mayer-Proschel, 1997), although the exact identity and fate potential of these cells in vivo are not yet clear. The observation (Franklin et al., 1995) that transplanted OPCs generate astrocytes in an astrocyte-free environment is also suggestive of an astroglial fate potential of NG2 glia.

In order to determine more directly the fate of NG2 glia, we have used the bacterial artificial chromosome (BAC) modification technique to generate transgenic mice that express the red fluorescent protein DsRed or the bacteriophage Cre recombinase specifically in NG2-positive (NG2+) cells. We show that NG2+ cells give rise to protoplasmic astrocytes as well as oligodendrocytes in vivo and in vitro.

MATERIALS AND METHODS

Generation of NG2DsRedBAC and NG2creBAC transgenic mice

We have used the BAC modification technique described by Heintz and colleagues (Yang et al., 1997; Heintz, 2001) to generate transgenic mice that express DsRed or Cre specifically in NG2-expressing cells (see Fig. S1 in the

[1]Department of Physiology and Neurobiology, University of Connecticut, 75 North Eagleville Road, Storrs, CT 06269-3156, USA. [2]Department of Neuroscience, Johns Hopkins University School of Medicine, 813 Wood Basic Science Building, 725 N. Wolfe Street, Baltimore, MD 21205, USA.

*Author for correspondence (e-mail: akiko.nishiyama@uconn.edu)

Table 1. Source and dilution of antibodies

Antibodies	Source	Dilution used
Primary		
Mouse anti-APC, clone CC1	Calbiochem	1:200
Mouse anti-CD31	BD Sciences	1:500
Rabbit anti-Cre	Novagen	1:5000
Rat anti-F4/80	Serotec	1:200
Rabbit anti-β-galactosidase	Eppendorf Five Prime	1:500
Mouse anti-GFAP	Sigma	1:1000
Rabbit anti-GFAP	DakoCytomation	1:1000
Guinea pig anti-GLAST	Chemicon	1:1000
Mouse anti-GFP	Chemicon	1:500
Rabbit anti-GFP	Chemicon	1:1000
Mouse anti-myelin basic protein (Smi99)	Sternberger Monoclonals	1:5000
Mouse anti-nestin	Chemicon	1:50-1:200
Mouse anti-NeuN	Chemicon	1:200
Rabbit anti-rat NG2	Dr W. Stallcup	1:1000
	Dr J. Levine	1:1000
	Chemicon	1:500
Guinea pig anti-rat NG2	Dr W. Stallcup	1:1000
Rat anti-mouse NG2	Dr J. Trotter	1:1000
Mouse anti-O4 and O1	Dr S. Pfeiffer	1:5 (supernatant)
Rabbit anti-PDGFRα	Dr W. Stallcup	1:1000
Rabbit anti-PDGFRβ	Dr W. Stallcup	1:1000
Mouse anti-S100β	Sigma	1:2000
Mouse anti-βIII-tubulin	Chemicon	1:200
Secondary		
FITC-, Cy3- and Cy5-conjugated anti-mouse, anti-rabbit, anti-rat and anti-guinea pig antibodies	Jackson ImmunoResearch	FITC 1:50 Cy3 1:200 Cy5 1:50
Alexa 488-conjugated anti-mouse or rabbit	Molecular Probes	1:2000

Materials were obtained from Dr W. Stallcup (La Jolla, CA), Dr J. Levine (Stony Brook, NY), Dr J. Trotter (Mainz, Germany) and Dr S. Pfeiffer (Farmington, CT).

supplementary material). We obtained a 208 kb BAC clone in pBACe3.6 vector from the RPCI-23 C57BL/6J mouse BAC library that contained the entire 33.97 kb *Cspg4* (*ng2*) gene (BACPAC Resources; Oakland, CA) in the center, flanked by 60,274 bp and 114,045 bp of additional sequences on the 5′ and 3′ ends of the gene, respectively. DsRed.T1 (Bevis and Glick, 2002) (a gift from Dr Benjamin Glick, University of Chicago, IL), which is a variant of the original red fluorescent protein DsRed1 derived from the coral *Discosoma* (Matz et al., 1999) with excitation and emission peaks at 554 and 586 nm, respectively, was inserted into the first exon of the *ng2* gene in the BAC clone as follows. An NG2-DsRed building vector was constructed in pBluescript by ligating together the following DNA fragments from 5′ to 3′: 555 bp of the 5′ NG2 homology arm, DsRed.T1 coding sequence, 535 bp of rabbit β-globin polyadenylation signal from pCAGGS (gift from Dr Kenji Sakimura, Niigata University, Japan), and 603 bp of NG2 3′ homology arm. The 5′ NG2 homology arm consisted of 542 bp upstream of the translation initiation codon and 33 bp downstream of the ATG. 5′-RACE analysis revealed the transcription initiation site to be 127 bp upstream from the translation initiation site (data not shown). DsRed.T1 was inserted into the first exon of the *ng2* gene after mutating the first translation initiation ATG to AAG to prevent translation from the BAC *ng2* gene and to allow translation from the first ATG in the DsRed.T1 cDNA in the context of a strong Kozak consensus sequence. The 3′ homology arm consisted of sequences in the first exon starting 4 bp downstream of the 5′ homology arm and extending 533 bp into the first intron (see Fig. S1A in the supplementary material).

The transgene was subcloned into pRecA.SV1 shuttle vector (provided by Dr Nathaniel Heintz, Rockefeller University, New York) that contains *recA* to allow homologous recombination (Yang et al., 1997). The resulting plasmid was used to transform DH10 competent cells harboring the NG2BAC DNA. The shuttle vector pRecA.SV1 contained a temperature-sensitive origin of replication and tetracycline resistance gene, which were used to screen colonies for integration and subsequent resolution events. The resulting modified BAC clones were analyzed by Southern blotting and PCR to confirm the integrity of the transgene and were further tested for adequate DsRed expression by transfecting N20.1 mouse oligodendrocyte precursor cells (Verity et al., 1993). DNA from a correctly modified clone was purified using the BAC Maxi kit (Clontech, Palo Alto, CA), linearized with *Not*I, and microinjected into the pronucleus of fertilized oocytes from B6SJL/F1 and C57BL/6J mice. Three founders were identified by PCR using primers from DsRed sequence.

A similar approach was used to generate NG2creBAC transgenic mice (see Fig. S1B in the supplementary material). The nls-cre cDNA that contains the coding region of cre with a nuclear localization signal was obtained from Dr Kenji Sakimura (Brain Research Institute, Niigata, Japan). This was used to generate an NG2creBAC building vector that was identical to the NG2DsRedBAC building vector except that the DsRed coding region was replaced with the nls-cre coding region.

Z/EG (lacZ/EGFP) Cre reporter mice (see Fig. S1B in the supplementary material) (Novak et al., 2000) were kindly provided to us by Dr Caiying Guo (University of Connecticut Health Center, Farmington, CT). Another Cre reporter mouse line, ROSA26R (Soriano, 1999), was obtained from the Jackson Laboratory (Bar Harbor, ME). These reporter lines were maintained as homozygous lines and crossed to NG2creBAC mice.

Tissue processing

Mice were anesthetized and sacrificed by intracardiac perfusion with 2% paraformaldehyde solution in phosphate buffer containing 0.01 M sodium metaperiodate and 0.1 M lysine (paraformaldehyde-lysine-periodate fix) (McLean and Nakane, 1974). Brain, cerebellum and spinal cord tissues were removed and postfixed for 2 hours in the same fixative followed by washes in 0.2 M sodium phosphate buffer (pH 7.4). Sections of 50 or 100 μm were cut on a Leica VT1000 Vibroslicer. Embryos were fixed by immersion fixation in the same fixative immediately after they were isolated from the uterus, rinsed in sodium phosphate buffer, cryoprotected in 20% sucrose, and 20 μm sections were cut on a cryostat (Microm HM 500M).
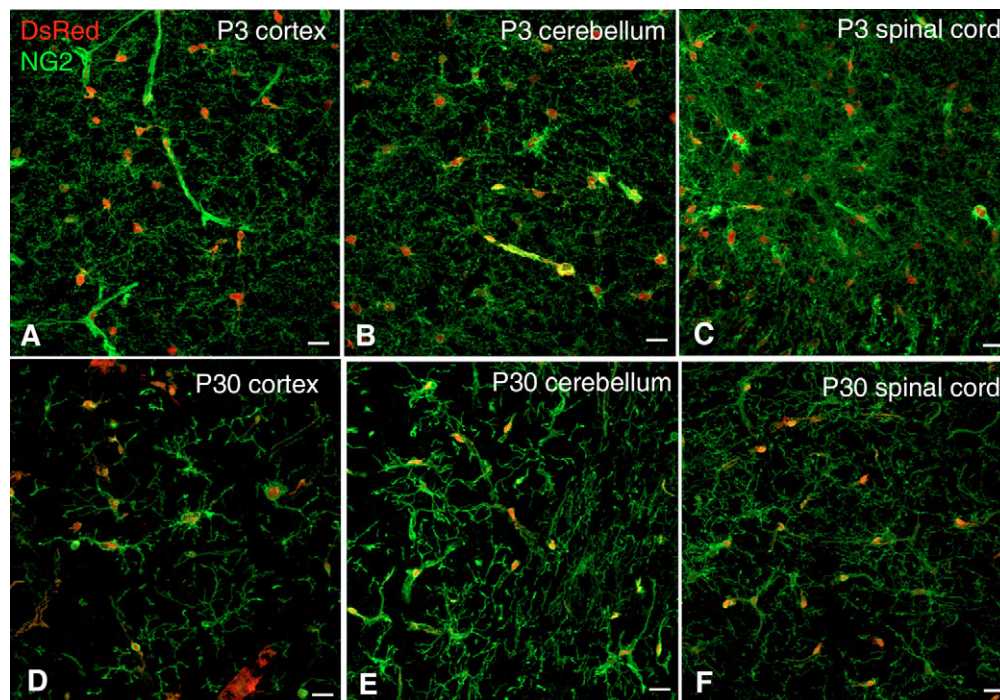
Fig. 1. Distribution of DsRed fluorescence and NG2 immunoreactivity in P3 and P30 tg cerebral cortex, cerebellum and spinal cord.
(**A**,**D**) Coronal sections through P3 (A) and P30 (D) cerebral cortex. (**B**,**E**) Sagittal sections through P3 (B) and P30 (E) cerebellum. (**C**,**F**) Transverse sections through P3 (C) and P30 (F) spinal cord. Vibratome sections (100 μm) were immunolabeled with anti-NG2 antibodies and Alexa Fluor 488 goat anti-rabbit immunoglobulins. DsRed fluorescence (red) is localized to the somata of NG2-immunoreactive (green) cells. DsRed+NG2+ cells are distributed uniformly throughout the CNS. Scale bars: 20 μm.

Fluorescence-activated cell sorting (FACS)

Cells were isolated from P2 or P3 wild-type (wt) and NG2DsRedBAC transgenic mouse (tg) brains by dissociating the cerebral cortex, subcortical white matter, and subventricular zone in S-MEM (Invitrogen, Carlsbad, CA) containing 0.1% trypsin and 50 μM kynurenic acid (Sigma, St Louis, MO) for 15 minutes at 37°C. Trypsin was inactivated by the addition of an equal volume of DMEM containing 10% fetal calf serum (FCS; Invitrogen). The cells were then triturated in the presence of 0.05 mg/ml of DNase I (Sigma). On average 1.2×10^6 cells were obtained from each cerebrum. The dissociated cells were subjected to FACS sorting using a Becton-Dickinson FACScalibur Dual Laser Flow Cytometer. Cells from wt and tg cerebra were used to establish the gate settings (Fig. 3). The electronic gain of the red channel was adjusted such that the maximum intensity of wt cells was designated as 10^1 on the *x*-axis of the flow cytometry data (Fig. 3B,D). Cells from tg cerebra were sorted at 1500-2500 cells per second. Sorted cells were collected by centrifugation, and plated on glass coverslips coated with 100 μg/ml poly-L-lysine. Cells were maintained in either neurobasal medium containing B27 supplements (Invitrogen) and 10 ng/ml platelet-derived growth factor (PDGF AA; R&D Systems, Minneapolis, MN), or neural stem cell medium consisting of DMEM-F12 containing 0.6% glucose, 3 mM sodium bicarbonate, 2 mM glutamine, 25 μg/ml insulin, 100 μg/ml transferrin, 20 nM progesterone, 60 μM putrescine, 30 nM sodium selenite 10 ng/ml FGF2 (fibroblast growth factor 2; R&D Systems), and 20 ng/ml EGF (epidermal growth factor; R&D Systems). In some experiments, cells from P3 subventricular zone (SVZ) or P5 cerebellum were dissociated as described above to obtain cultures of neural stem cells or neurons.

Immunolabeling

Immunohistochemistry

Immunohistochemistry was performed as described previously (Bu et al., 2001; Bu et al., 2004). The source and dilution of the antibodies are listed in Table 1. Labeled sections were mounted in Vectashield containing DAPI (Vector) and examined using a Leica DMR epifluorescence upright microscope equipped with a digital camera (ORCA, Hamamatsu, Japan) and

the IP Lab image acquisition software (Scanalytics, Fairfax, VA), Zeiss Axiovert 200M equipped with Axiocam and ApoTome, or with a Leica TCS SP2 spectral confocal imaging system.

Immunocytochemistry

Cell surface antigens were detected by live cell staining. Coverslips were incubated in DMEM containing 10% serum (DMEM-10F) and primary antibodies (listed in Table 2) diluted in DMEM-10F at room temperature for 30 minutes. Following brief rinsing in DMEM-10F, cells were incubated in secondary antibodies for 30 minutes at room temperature. Following three rinses in DMEM-10F, the cells were fixed for 10 minutes in 4% paraformaldehyde, washed three times, 5 minutes each, in PBS, and mounted in Vectashield containing DAPI.

To reveal intracellular antigens, cells were first fixed in 4% paraformaldehyde for 10 minutes, washed three times in PBS, permeabilized and blocked in DMEM containing 5% normal goat serum and 0.1% Triton X-100 for 30 minutes at room temperature. Then the cells were incubated in antibodies to intracellular antigens for 30 minutes at room temperature. After three washes in PBS, for 5 minutes each, the cells were incubated in secondary antibodies for 30 minutes at room temperature, washed three times in PBS, and mounted as above.

Cell counts

For antigenic phenotyping of sorted cells, the number of cells that were immunopositive for each antigen was counted and expressed as a percentage of all DAPI+ cells. At least 150 cells were scored on each coverslip, and a minimum of three coverslips from three independent sorting experiments were analyzed. The numbers were expressed as means ± standard deviations.

To assess regional differences in the number of astrocytes generated from NG2 glia, the number of cells that were immunoreactive for EGFP or S100β was counted in one hemisphere from three P14 NG2creBAC:Z/EG double tg brains. Using a 20× objective lens, the optical fields were systematically scanned from dorsal to ventral cortex or from dorsolateral striatum to the ventral midline, and the number of cells that were EGFP+ or S100β+ was
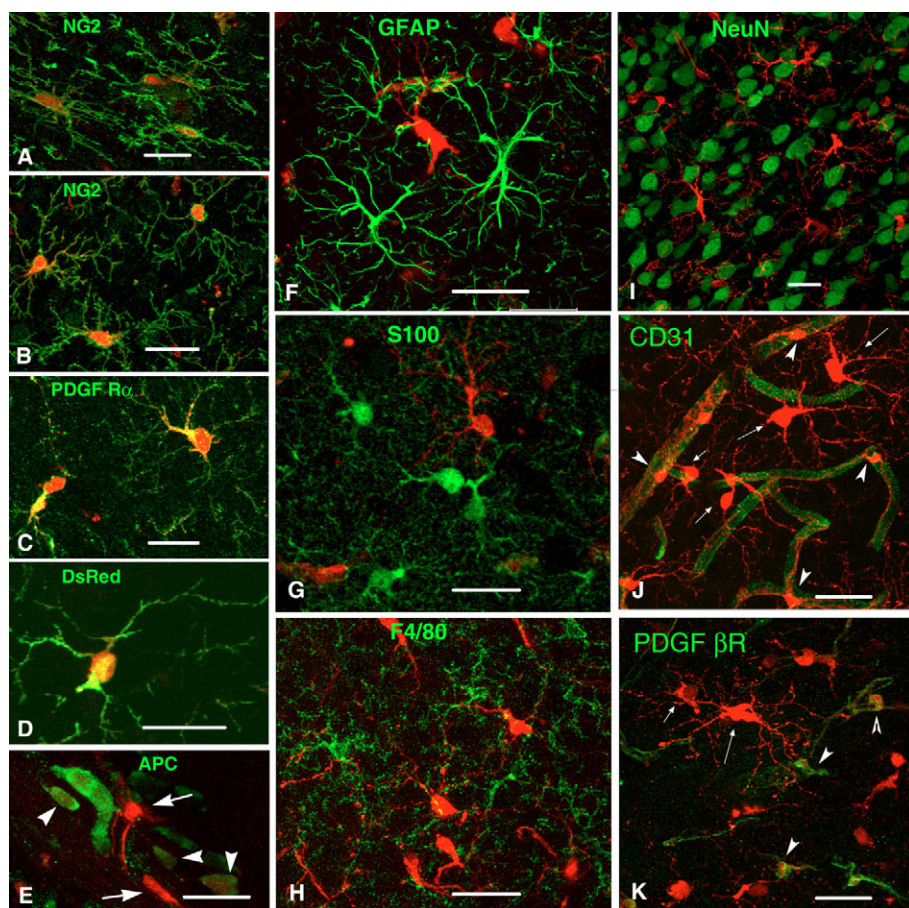
148   RESEARCH ARTICLE

Development 135 (1)

Fig. 2. Cellular localization of DsRed in coronal sections of P30 tg brain. (**A**,**B**) DsRed fluorescence (red) is detected in all the cells that are NG2+ (green) in corpus callosum (A) and cerebral cortex (B). (**C**) All the cells exhibiting DsRed fluorescence in the cerebral cortex express PDGFRα+ (green). (**D**) Comparison of DsRed fluorescence (red) and DsRed protein detected by a rabbit anti-DsRed antibody (green) in the cerebral cortex. DsRed protein is detected in the soma and throughout the processes. (**E**) Comparison of DsRed fluorescence with the oligodendrocyte antigen APC (green) in the corpus callosum. Strongly DsRed+ cells are negative for APC (arrows), whereas some weakly DsRed+ cells are APC+ (arrowheads). (**F**,**G**) DsRed fluorescence is not detected in astrocytes expressing GFAP (F) or S100β (G) in the cerebral cortex. (**H**) DsRed fluorescence is not detected in F4/80+ microglia in the cerebral cortex. (**I**) DsRed fluorescence is not detected in NeuN+ neurons in the cerebral cortex. Yellow indicates regions of contact, but the two antigens are not present in the same cells. (**J**,**K**) DsRed fluorescence is detected in PDGFRβ+ pericytes (K, arrowheads) but not in CD31+ endothelial cells (J, arrowheads) in the cerebral cortex. Scale bars: 12.5 μm in A-C; 20 μm in D,E; 25 μm in F-K.

counted. The density of cells was determined by dividing the total number of cells by the total area of the scanned fields. Area measurements were obtained using the Axiovision program on Zeiss Axiovert 200M.

RESULTS
NG2+ cell-specific expression of DsRed in NG2DsRedBAC transgenic mice
DsRed is expressed specifically in NG2-expressing cells
The BAC modification approach was taken to ensure inclusion of all the regulatory sequences needed for NG2 cell-specific expression of the transgene, particularly those in the large first intron spanning 18.3 kb. DsRed was expressed specifically in NG2+ cells in all of the three identified founder lines. The line with the highest level of expression was used for all of the experiments described below. We detected no evidence for gene rearrangement within the BAC sequences by Southern blotting. No overt alterations were found in the cytoarchitecture of the brains from wild-type (wt) and transgenic (tg) mice.

The distribution of DsRed fluorescence in NG2DsRedBAC tg mice was compared with NG2 immunoreactivity in postnatal day 3 (P3) and P30 tg mice (Fig. 1). DsRed+NG2+ cells were distributed widely throughout the gray and white matter of the brain, cerebellum and spinal cord, with the exception of the external granule cell layer of the P3 cerebellum, which was devoid of DsRed+NG2+ cells (not shown). In addition to glial cells, vascular mural cells also expressed DsRed (see below). The distribution of DsRed+ and NG2-immunoreactive cells overlapped in all the regions examined at both developmental stages. DsRed fluorescence was sufficiently strong that it could be readily detected without using anti-DsRed antibodies.

The expression of DsRed was more closely compared with that of various cell type-specific markers in the P30 brain. In the cerebral cortex and corpus callosum, all NG2-immunoreactive cells contained DsRed fluorescence (Fig. 2A,B). DsRed fluorescence was most intense in the cell bodies but was also detected in distal processes (Fig. 2D), suggesting that the tetrameric DsRed.T1 mutant used in the current study (Bevis and Glick, 2002) remains soluble and does not aggregate as much as the original DsRed protein (Yarbrough et al., 2001).

DsRed is expressed in cells of the oligodendrocyte lineage
In P30 tg mouse brain, all the DsRed+ non-vascular cells in both gray and white matter expressed PDGFRα (Fig. 2C), an antigen known to be expressed by NG2+ OPCs (Pringle et al., 1992; Nishiyama et al., 1996a; Nishiyama et al., 1996b). DsRed+ vascular cells were negative for PDGFRα. To determine whether DsRed was expressed by mature oligodendrocytes, sections from P30 tg brains were labeled with a monoclonal antibody to the *adenomatosis polyposis coli* (*Apc*) gene product (clone CC1) which was previously shown to be expressed by mature oligodendrocytes (Bhat et al., 1996). In the corpus callosum, APC+ oligodendrocytes were clustered in rows parallel to the orientation of axons and had characteristic large oval cell bodies (Fig. 2E). Strongly DsRed+ cells were negative for APC (Fig. 2E, arrows). However, there were some APC+ cells with typical oligodendroglial morphology that had dim DsRed fluorescence (Fig. 2E, arrowheads), suggesting that DsRed expression persists in immature oligodendrocytes. Since there was little overlap between NG2+ and APC+ cells (data not shown), it appears that DsRed expression is downregulated after the
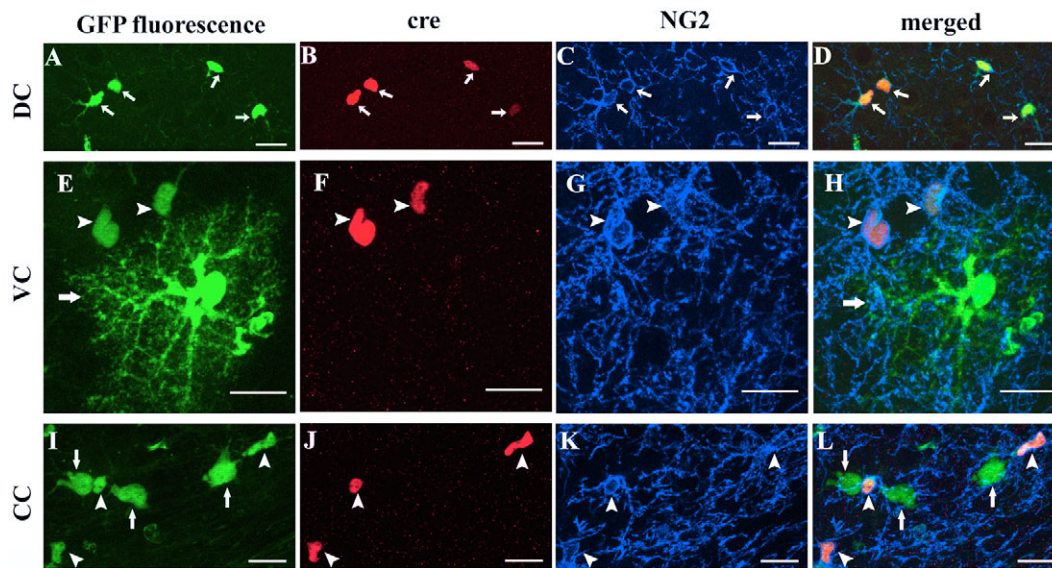
Fig. 3. Cre expression in NG2creBAC:Z/EG double tg mice. Coronal sections (50 μm) through dorsal and ventral cortex and corpus callosum from a P14 double tg mouse were double labeled with rabbit anti-Cre (red in B,D,F,H,J,L) and guinea pig anti-NG2 (blue in C,D,G,H,K,L) antibodies. (**A-D**) In dorsal cortex (DC) Cre is expressed in NG2+ cells with EGFP fluorescence (arrows). (**E-H**) In ventral cortex (VC) Cre is expressed in NG2+ cells with EGFP fluorescence (arrowheads), but not in EGFP+ protoplasmic astrocytes, which are devoid of NG2 (arrows). (**I-L**) In the corpus callosum (CC) Cre is expressed in NG2+ cells with EGFP fluorescence (arrowheads), but not in EGFP+NG2– oligodendrocytes with large cell bodies and few short and thick processes (arrows). Cre is only present in NG2+ cells and not in EGFP-expressing astrocytes or oligodendrocytes in NG2creBAC:Z/EG double tg mouse. Scale bars: 20 μm.

disappearance of NG2, which may reflect a longer half-life of DsRed protein compared to that of NG2. We did not observe any myelin that had DsRed fluorescence.

DsRed is not expressed by astrocytes, microglia or neurons in P30 brain

Sections from P30 tg brains were labeled with antibodies to cell type-specific antibodies to examine the expression of DsRed in cells other than oligodendrocytes lineage cells. DsRed was not detected in astrocytes that were immunoreactive for glial fibrillary acidic protein (GFAP) or S100β (Fig. 2F,G). Neither was there any overlap between DsRed+ cells and F4/80+ resting ramified microglia (Fig. 2H). In P30 cerebral cortex, DsRed+ cells were dispersed among the numerous NeuN+ neurons (Fig. 2I). However, there was no co-expression of NeuN and DsRed by the same cells, even in the neurogenic regions of the hippocampus and olfactory bulb (not shown).

DsRed is present in mural cells of the cerebral vasculature

In addition to glial cells, DsRed was expressed on vascular cells, as previously reported for NG2 (Ozerdem et al., 2001). To investigate the expression of DsRed in the vasculature, we used antibodies to CD31 (also known as PECAM1) to detect endothelial cells (Vecchi et al., 1994) and PDGFRβ to detect vascular mural cells, which include pericytes and smooth muscle cells (Ozerdem et al., 2001). Labeling of P30 tg brain sections with antibodies to CD31 revealed the contour of the capillaries. DsRed+ cells with long slender processes were seen along the outer perimeter of the capillaries, and their processes seemed to surround the surface of the blood vessels (Fig. 2J, arrowheads). All of the vascular DsRed+ cells in the P30 tg brain were immunopositive for PDGFRβ (Fig. 2K, arrowheads). DsRed+ vascular cells were morphologically different from parenchymal glial cells (arrows in Fig. 2J,K). Vascular DsRed+ cells had smaller, round cell bodies with fewer processes that appeared

thicker and 'fuzzier' than those of DsRed+ glial cells. Vascular expression of DsRed and NG2 was more prominent at P3 (Fig. 1A,C,E) than at P30 (Fig. 1B,D,F). The distribution of DsRed+ cells described here demonstrates the highly tissue-specific expression of DsRed in the NG2DsRedBAC tg mouse brain that is restricted to NG2-expressing cells.

Fate of NG2+DsRed+ cells in vitro
Optimization of cell sorting conditions

Pilot experiments were performed to optimize the gating parameters for sorting DsRed+ cells from NG2DsRedBAC tg brains. For plots of cells from wt and tg brains, see Fig. S2 in the supplementary material. Gates for forward and side scatter were adjusted to exclude small dead cells and large cells with granular cytoplasm that were likely to be macrophages with autofluorescence (see Fig. S2C in the supplementary material). Gates M1, M2 and M3 were set with increasing stringency to collect cells with relative fluorescence intensity greater than 10, 50 and 100, respectively (see Fig. S2D in the supplementary material). In wt cells the fluorescence intensity in the red channel was less than 10. Sorted cells were plated on poly-L-lysine-coated coverslips. The presence of DsRed fluorescence in the sorted cells was scored 2 hours after plating using a Leica DMR upright epifluorescence microscope. The percentage of DsRed+ cells among cells sorted with gates M1, M2 and M3 were 87.4%, 91.3% and 97.8%, respectively. Upon close inspection of the cells sorted with the M3 gate, all of the DsRed-negative (DsRed–) cells had nuclei that were either apoptotic or were enlarged and diffuse, without a well defined nuclear membrane. Such unhealthy-looking DsRed-negative cells were not detected 4 hours after plating, suggesting that they had not adhered to the coverslips and died during the additional 2 hours of incubation. When the coverslips were scored 4 hours after sorting, 100% of the DAPI+ cells sorted
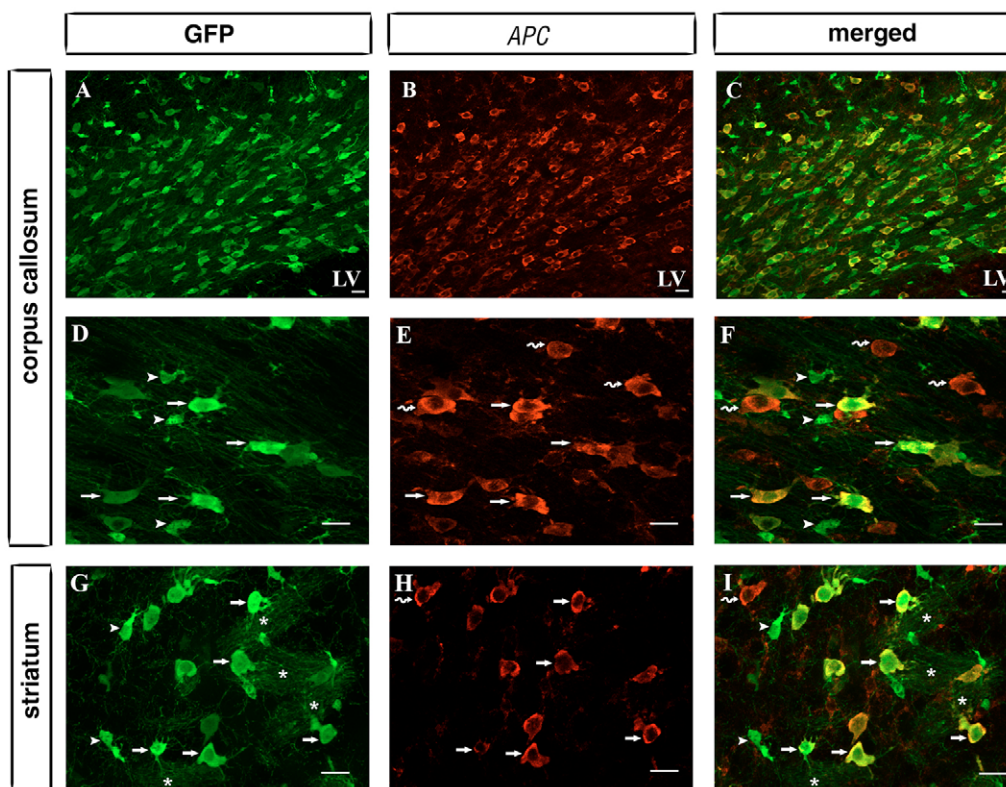
Fig. 4. EGFP is expressed in APC+ oligodendrocytes and myelin in the white matter of P14 NG2CreBAC:Z/EG double tg mouse. Coronal sections (50 μm) through corpus callosum or striatum from P14 double tg mouse were double labeled with rabbit anti-EGFP (A,D,G; green), and mouse anti-APC (B,E,H; red) antibodies. (**A-C**) Projected images of z-stacks from the corpus callosum. The distribution of EGFP+ cells is similar to that of APC+ cells with extensive overlap between EGFP and APC. (**D-I**) Higher magnification of projected images of z-stacks from the corpus callosum (D-F) and striatum (G-I). APC+ oligodendrocytes in the corpus callosum express EGFP (straight arrows). EGFP-expressing NG2 glia are negative for APC (arrowheads). Some of the APC+ oligodendrocytes do not express EGFP (wavy arrows). EGFP+ oligodendrocytes form myelin, which is also EGFP+ (asterisks). Scale bars: 20 μm.

through the M3 gate exhibited visible DsRed fluorescence (see Fig. S3 in the supplementary material). Therefore, all of the subsequent sorting experiments were performed using the M3 gate.

Antigenic phenotype of sorted cells

The antigenic phenotype of the sorted cells was determined by immunolabeling adhered cells with antibodies to NG2, PDGFRα, the newly differentiated oligodendrocyte antigen O1, GFAP and βIII-tubulin 4 hours after plating (see Fig. S3 in the supplementary material). At this time point, most of the cells had adhered, and short processes could be detected on some cells, while the majority of the cells remained round. After NG2 and PDGFRα were cleaved from the cell surface during dissociation, punctate immunoreactivity for these antigens was clearly discernible at the cell surface by 4 hours after plating (see Fig. S3C,F in the supplementary material). A small number of cells expressed O1 (see Fig. S3I in the supplementary material). For the percentage of cells that were immunoreactive for each antigen, see Fig. S4E in the supplementary material. More than 98% of the cells expressed NG2 at the cell surface, and 1-5% of the cells were O1+. Together, NG2+ and O1+ cells accounted for all of the cells, and a small number of cells weakly expressed both NG2 and O1, as previously described for secondary NG2 cell cultures from the cerebrum (Nishiyama et al., 1996b) (see also Fig. S4D in the supplementary material). The percentage of O1+ cells at 4 hours increased with the age of the mice from which the cells were isolated. The majority of the sorted cells expressed PDGFRα (see

Fig. S3D-F in the supplementary material), and none were PDGFRβ+ (data not shown), indicating that the isolated cells were predominantly of the oligodendrocyte lineage and not of vascular mural origin. None of the sorted cells expressed the neuronal markers βIII-tubulin or NeuN.

Differentiation of sorted cells

To determine the differentiation potential of NG2-expressing cells, DsRed+ cells were sorted from P3 brains by FACS. The dissected material included cerebral cortex, subcortical white matter, corpus callosum, subventricular zone (SVZ), and hippocampus but did not include the basal ganglia or diencephalon. Typically, three transgenic mouse brains were used for each FACS experiment with a yield of $1\sim2\times10^6$ cells from each brain. Sorting conditions were carefully established to yield 100% DsRed+ cells as determined by fluorescence microscopy 4 hours after plating. Immunolabeling of the sorted cells showed that NG2+ cells and O1+ cells accounted for all of the sorted cells (see Figs S2, S3 in the supplementary material).

Oligodendrocyte lineage cells

Differentiation potential of the sorted cells was determined by culturing them in neurobasal medium plus B27 and PDGF AA for 4 days, followed by incubation in neurobasal medium plus B27 without PDGF AA for 7 days, and examining their antigenic phenotype after 4, 7 and 11 days. For the percentage of cells that were immunoreactive for each antigen after 4 and 11 days in vitro
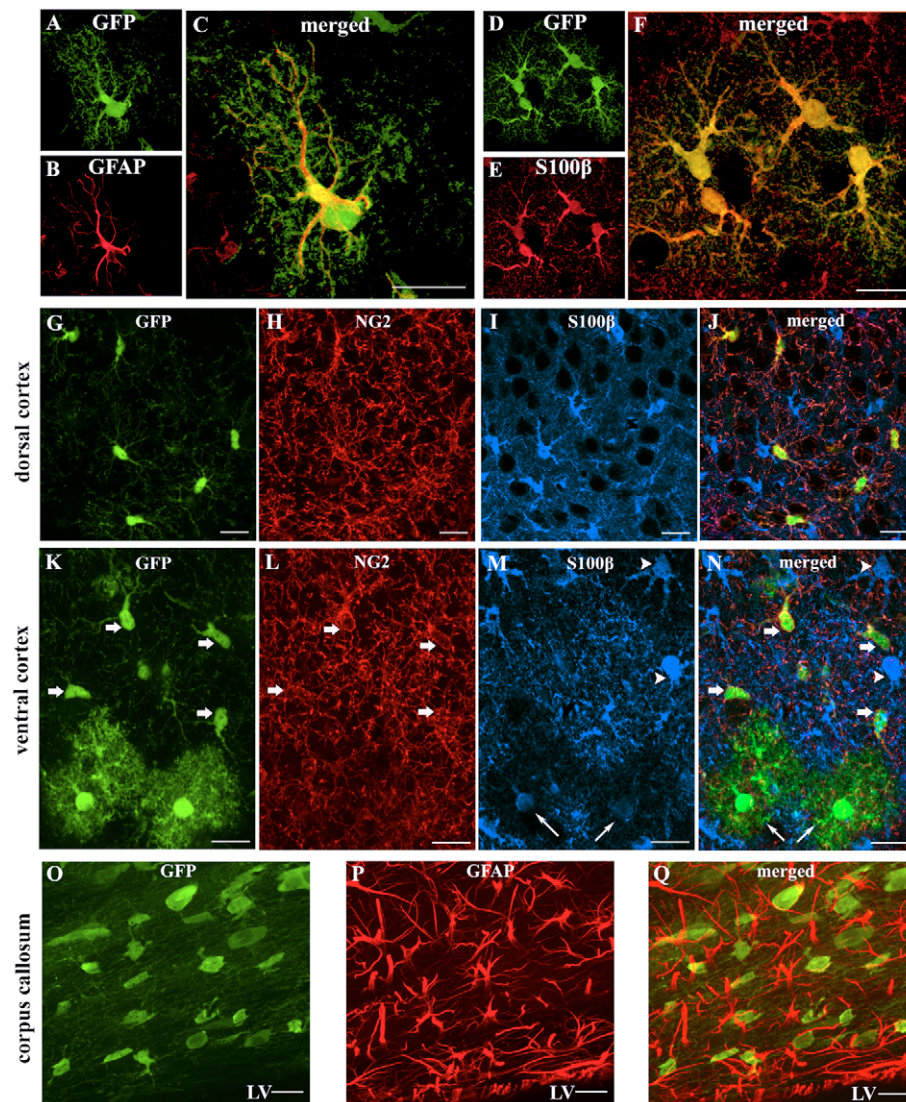
Fig. 5. EGFP+ astrocytes in ventral but not dorsal cortex of P14 NG2CreBAC:Z/EG tg mice. Coronal sections (50 μm) through dorsal and ventral cortex and corpus callosum from P14 double tg mice were double or triple labeled with rabbit anti-EGFP (green in A,C,D,F,G,J,K,N,O,Q), mouse anti-GFAP (red in B,C,P,Q), mouse anti-S100β (red in E,F; blue in I,J,M,N), and guinea pig anti-NG2 (red in H,J,L,N) antibodies. (**A-F**) High magnification of EGFP+ astrocytes in ventral cortex. EGFP+ cells that have the typical morphology of protoplasmic astrocytes with bushy processes are immunoreactive for GFAP (A-C) or S100β (D-F). (**G-J**) EGFP+ cells in dorsal cortex are immunoreactive for NG2. S100β+ protoplasmic astrocytes in dorsal cortex are negative for NG2 and EGFP. (**K-N**) EGFP+ cells in ventral cortex extending bushy processes characteristic of protoplasmic astrocytes are also immunoreactive for S100β (thin arrows in M and N). EGFP+ NG2 cells are positive for NG2 but devoid of S100β (thick arrows). Some S100β+NG2– cells do not express EGFP (arrowheads). (**O-Q**) None of the EGFP+ cells in the corpus callosum express GFAP. Yellow areas represent overlap of GFAP and APC from adjacent cells, but the two antigens are never present in the same cells. Scale bars: 20 μm.

(div), see Fig. S4E in the supplementary material. At 4 and 7 div, the majority of the cells were NG2+ and PDGFRα+ (see Fig. S4A,B in the supplementary material), but there were also differentiated O1+ oligodendrocytes with expansive membranous processes (see Fig. S4C in the supplementary material). The majority of the cells (>85%) were NG2+ even after 11 div; some appeared relatively immature whereas others were multipolar and resembled immature oligodendrocytes (see Fig. S4D in the supplementary material). Under these conditions, O1+ cells constituted less than 20% of the population in most experiments. Culturing the cells for longer periods of time did not result in a significant increase in the number of O1+ cells above 15%. There were signs of cell death among O1+ cells, suggested by the presence of remnants of O1+ membranes that were unaccompanied by DAPI+ nuclei, and by condensed nuclei. NG2+ cells and O1+ cells together accounted for the majority of the cells at 4 and 11 days after plating.

GFAP+ cells

By 4 div, a small number of NG2 cells had a morphology that was distinct from that of oligodendrocyte progenitor cells. These cells had either multiple processes that appeared thicker than those of OPCs, resembling those of type 2 astrocytes, or were flat and pancake-shaped (see Fig. S4E in the supplementary material). Both types of NG2+ cells showed filamentous GFAP immunoreactivity in the cytoplasm. Such NG2+GFAP+ cells increased in number over time, and by 11 div, they constituted more than 20% of the population (see Fig. S3E in the supplementary material). There was a spectrum of intensity of NG2 and GFAP immunoreactivity among both flat and process-bearing cells (see Fig. S4F in the supplementary material). Until 7 div, 100% of the GFAP+ cells expressed surface NG2. After 11 div, some flat GFAP+ cells did not express NG2 (see Fig. S4G in the supplementary material). These GFAP+NG2– cells coexisted in the same cluster with flat pancake-shaped GFAP+NG2+ cells. To determine whether GFAP+NG2+ cells were lineally related to the vascular mural cells, cells were immunolabeled for GFAP and PDGFRβ. There was no detectable PDGFRβ on the surface of GFAP+ cells (see Fig. S4H in the supplementary material), whereas immunoreactivity for PDGFRβ was clearly detected on GFAP-negative cells in total brain cell cultures used as positive control for PDGFRβ labeling (see Fig. S4I in the supplementary material).

Neuronal lineage

To determine whether DsRed+ cells could be induced to differentiate into neurons, sorted DsRed+ cells were cultured in neural stem cell (NSC) medium previously used by Belachew et al. (Belachew et al.,

Table 2. Distribution of NG2-cell-derived astrocytes in the forebrain

A. Anterior forebrain*

Brain region	Dorsal cortex	Ventral cortex	Striatum
Area (mm^2)	3.87±0.79	2.63±0.82	2.58±0.75
Total number of S100β+ cells	1378.7±179.0	1255.0±481.1	1113.0±381.7
Total number of GFP+ cells	1447.3±268.7	996.0±329.4	958.0±237.7
Total number of GFP+S100β+ astrocytes‡	21.3±5.9	217.7±57.0	107.7±61.8
Density of GFP+S100β+ astrocytes‡ (/mm^2)	5.7±2.1	84.5±17.3	39.7±18.5
% GFP+S100β+ cells/total S100β+ cells§	1.6±0.4	18.0±4.1	9.1±3.6
% S100 β+ cells/total GFP+ cells¶	1.6±0.7	22.3±4.4	10.6±4.9

B. Posterior forebrain†

| Brain region	Dorsal cortex	Ventral cortex	Striatum	Hippocampus
Area (mm^2)	1.64±0	0.99±0.086	0.89±0	0.60±0
Total number of S100β+ cells	817.3±59.5	514.3±109.5	536.3±37.3	428.3±42.9
Total number of GFP+ cells	750.3±90.4	448.7±44.6	506.3±0.6	300.0±27.2
Total number of GFP+S100β+ astrocytes‡	8.0±4.0	186.3±36.5	94.0±8.9	37.3±16.9
Density of GFP+S100β+ astrocytes‡ (/mm^2)	4.9±2.4	186.7±22.0	105.3±9.9	62.7±28.4
% GFP+S100β+ cells/total S100β+ cells§	1.0±0.5	36.3±2.5	17.6±2.7	8.7±3.5
% S100 β+ cells/total GFP+ cells¶	1.1±0.5	41.4±6.3	18.6±1.8	12.2±4.5

*Anterior forebrain: level of anterior commissure (see diagram below).
†Posterior forebrain: level of dorsal hippocampus (see diagram below).
‡The number of NG2 cell-derived astrocytes was estimated by counting the number of GFP+ cells that were also S100β+ and had the typical appearance of protoplasmic astrocytes with bushy processes.
§The proportion of S100β+ astrocytes that were derived from NG2 cells.
¶The proportion of NG2 cell-derived astrocytes among all NG2 cell progeny.
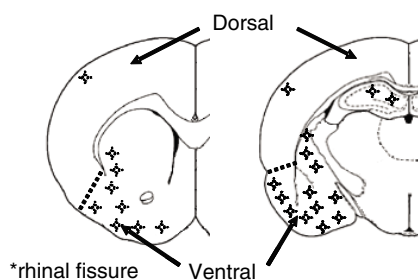
2003) to achieve differentiation of neurons from *cnp* promoter-EGFP tg cells. When DsRed+ cells from P3 brains were maintained in NSC medium in the presence of FGF2 and EGF for 4 days, followed by 7 days of incubation in the absence of growth factors, we did not detect any βIII-tubulin+ cells (see Fig. S4J in the supplementary material). βIII-tubulin could be readily detected on cerebellar granule neurons cultured from P5 mice (see Fig. S4K in the supplementary material). These findings suggest that FACS-sorted NG2+DsRed+ cells are primarily of glial lineage and do not give rise to neurons under these conditions.

Fate of NG2 cells in mice double transgenic for NG2creBAC and Z/EG
NG2creBAC transgenic mice
To determine whether NG2 glia give rise to astrocytes in vivo, we generated NG2creBAC tg mice (see Fig. S1B in the supplementary material) by using the same strategy that we had used to generate the NG2DsRedBAC tg mice, and replaced DsRed cDNA with nls-cre cDNA, which encodes Cre with a nuclear localization signal (obtained from Dr Kenji Sakimura; Brain Research Institute, Niigata University). In the NG2creBAC tg mouse line, Cre immunoreactivity was detected exclusively in NG2-expressing cells at all ages examined (P1, P14 and P60) (Fig. 3) and was not detected in S100β+ or GFAP+ astrocytes or in APC+ oligodendrocytes. To follow the progeny of NG2 glia, we crossed the NG2creBAC tg mice with Z/EG reporter mice (see Fig. S1B in the supplementary

material) (Novak et al., 2000). In NG2creBAC:Z/EG double tg mice, cells that have undergone Cre-mediated excision can be distinguished by those that have not by the expression of EGFP in the former and β-galactosidase in the latter. When double-tg mice were analyzed at P1, P14 and P60, EGFP was expressed in the majority of NG2+ cells throughout the brain at all time points examined. At P14, 86% of NG2+ cells expressed EGFP in the double tg mice. A small percentage of NG2+ cells expressed Cre but not EGFP, which indicates that the efficiency of Cre-mediated recombination was less than 100%.

Myelinating oligodendrocytes are generated from NG2 glia
To determine whether NG2 glia generate myelinating oligodendrocytes in vivo, we analyzed NG2creBAC:Z/EG double tg mice at P14, when myelination is actively occurring in the forebrain. Oligodendrocytes and EGFP+ cells were identified by antibodies to APC and GFP, respectively. In white matter tracts, EGFP was detected not only in NG2+ cells but also in NG2-negative cells that displayed a typical oligodendrocyte morphology, with large, round cell bodies, which were also APC+. The distribution of such EGFP+ cells in the corpus callosum and white matter of the striatum was similar to that of APC+ oligodendrocytes, and there was extensive colabeling of the same cells (Fig. 4A-C). In the corpus callosum and fiber tracts in the striatum, 77.8% of the APC+ oligodendrocytes expressed EGFP, indicating that these APC+EGFP+ oligodendrocytes had been generated from NG2 glia. A small number of APC+ oligodendrocytes
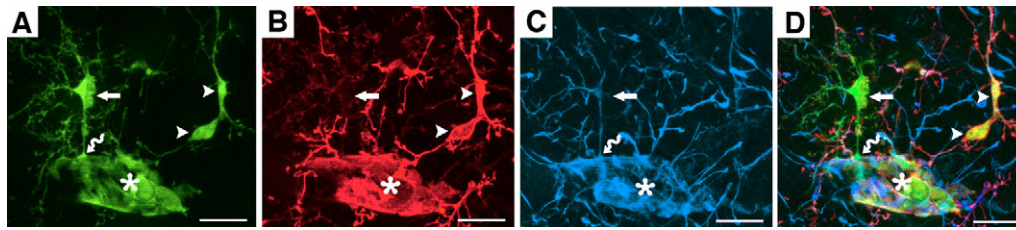
Fig. 6. NG2 cell-astrocyte transition in P1 NG2creBAC:Z/EG double tg mice. (**A-D**) Coronal sections (50 μm) through ventral cortex from a P1 double tg mouse were triple labeled with rabbit anti-EGFP (green in A,D), guinea pig anti-NG2 (red in B,D) and mouse anti-nestin (blue in C,D) antibodies. An EGFP+nestin+ cell (straight arrows) with protoplasmic astrocytic morphology and weak NG2 expression extends a process with a broad end-foot (wavy arrows) that contacts a blood vessel (asterisks). Two typical NG2 glia on the right with strong NG2 expression (arrowheads) do not have vascular end-feet. Scale bars: 20 μm.

were EGFP–. EGFP was also detected in myelinating processes of the oligodendrocytes (Fig. 4D-I). EGFP-labeled myelin was seen more abundantly in the NG2creBAC:Z/EG double tg mice at P60 than at P14. These findings indicate that NG2 glia give rise to myelinating oligodendrocytes in the postnatal brain.

Protoplasmic astrocytes in ventral forebrain gray matter are generated from NG2 cells

In the brains from P14 NG2creBAC:Z/EG double tg mice, we observed a significant number of EGFP+ cells with the typical morphology of protoplasmic astrocytes, which were more prevalent in the ventrolateral gray matter than in the neocortex (Fig. 5). EGFP+ astrocytes were mainly located in the ventral forebrain including the temporal cortex, ventrolateral striatum, septum, hippocampus and thalamus, and most were immunoreactive for S100β but not for NG2 (Fig. 5D-F,K-N). A small proportion of the EGFP+ cells with astrocytic morphology were S100β-negative. A subpopulation of EGFP+ astrocytes at the border between the ventral cortex and striatum also expressed GFAP (Fig. 5A-C), whereas many of the other EGFP+ astrocytes were GFAP–. EGFP+ astrocytes often appeared in clusters (Fig. 5D,K), and some of the EGFP+ astrocytes were found in close proximity to EGFP+ myelinating oligodendrocytes. Very few EGFP+S100β+ protoplasmic astrocytes were found in the dorsal cortex (Fig. 5G-J). In contrast to the gray matter, none of the EGFP+ cells in the corpus callosum expressed GFAP (Fig. 5O-Q), and EGFP+ cells in white matter were either NG2+ cells or APC+ oligodendrocytes.

To determine the prevalence of NG2 glia-derived astrocytes, we counted the number of EGFP+ and S100β+ cells in different regions of 50 μm coronal sections from P14 NG2creBAC:Z/EG double tg mice. Cell counts were obtained from coronal sections through the anterior forebrain at the level of anterior commissure (Table 2A) and from sections through the posterior forebrain at the level of dorsal hippocampus (Table 2B). S100β was used as a marker to count astrocytes, since GFAP was not detectable in the majority of protoplasmic astrocytes. The number of EGFP+S100β+ astrocytes was determined by counting cells that were positive for both EGFP and S100β and displayed the typical morphology of protoplasmic astrocytes. There were some S100β+EGFP+ cells that were myelinating oligodendrocytes, and they were excluded from the counts. In ventral cortex of anterior forebrain (see diagram in Table 2 for definition of dorsal and ventral cortex used here), 18% of the S100β+ cells were EGFP+ astrocytes, and 22% of all the EGFP+ cells had astrocytic morphology. The percentage of EGFP+ astrocytes out of all S100β+ cells was two-fold greater in the ventral gray matter regions from posterior forebrain than in the corresponding ventral region of the anterior forebrain. More than one-third of S100β+ cells

in posterior ventrolateral cortex were EGFP+. Considering that a small proportion of S100β+ cells were oligodendrocytes, the proportion of astrocytes in this region that were EGFP+ is likely to be higher. The density of EGFP+ astrocytes in dorsal cortex was 10- to 30-fold lower than that in ventral forebrain (see diagram in Table 2 for the designation of ventral and dorsal regions). Taken together, these findings indicate that NG2 glia differentiate into protoplasmic astrocytes primarily in the ventral gray matter of the forebrain, and that they do not generate fibrous astrocytes in white matter.

A similar pattern of distribution was found in P60 NG2creBAC:Z/EG double tg mice. EGFP+ astrocytes were also observed when another line of NG2creBAC transgenic mice was crossed to the Z/EG reporter line. In order to rule out the possibility that the ventral distribution of NG2 cell-derived protoplasmic astrocytes was due to the region-dependent expression of the reporter gene in Z/EG mice, we examined P14 Z/EG mice for the expression of the reporter and found that β-galactosidase was expressed similarly in both dorsal and ventral glial cells. Furthermore, when NG2creBAC tg mice were crossed to ROSA26R reporter mice in which the expression of the Cre reporter β-galactosidase is under an entirely different universally active promoter, a similar predominance of reporter expression in ventral telencephalic astrocytes was observed. These observations indicate that the higher frequency of NG2 cell-derived astrocytes in the ventral telencephalon is probably due to greater astrocyte differentiation from NG2 glia in ventral forebrain and not due to an uneven distribution of reporter expression.

At P1, some NG2-negative EGFP+ cells were already found in the ventral telencephalic gray matter of NG2creBAC:Z/EG double tg mice. The EGFP+NG2– cells did not express S100β or GFAP but expressed nestin and had multiple slender processes, and are likely to be immature astrocytes. Some EGFP+ cells that were weakly nestin+ had processes that appeared bushy in the distal regions. Weak NG2 expression was detected in such cells, especially at the tips of some of their processes (Fig. 6). Some of the EGFP+nestin+NG2+ 'immature' astrocytes extended processes that terminated on blood vessels with a web-like ending (Fig. 6A, curved arrow), resembling the vascular end-foot of an astrocyte. At P14, a spectrum of different intensities of NG2 immunoreactivity was observed among the EGFP+ cells, and those with weaker NG2 labeling had bushier processes resembling those of protoplasmic astrocytes. These findings are indicative of a transition from NG2 glia to NG2-negative protoplasmic astrocytes in the ventral gray matter of the postnatal brain.

Such transitional forms were already evident at embryonic day 18 (E18). A cluster of EGFP+ cells was found in the ventral forebrain close to the ventral pial surface (Fig. 7B,E,F). The majority of the EGFP+ non-vascular cells expressed NG2 and had a relatively small

number of long, slender processes. Some EGFP+ cells in the ventral forebrain had little or no detectable NG2 and expressed GLAST (glutamate aspartate transporter), known to be expressed by immature astrocytes (Fig. 7B,F). Such EGFP+GLAST+ cells were more abundant in the posterior (Fig. 7F) than anterior (Fig. 7B) ventral forebrain and were not detected in the dorsal forebrain at this age. They were found in close proximity to the cluster of EGFP+NG2+ cells. Some of the EGFP+GLAST+ cells, particularly those in the posterior ventral forebrain, had highly branched processes and morphologically resembled immature protoplasmic astrocytes seen in the early postnatal double tg brain (Fig. 7F, inset).

Absence of NG2 or EGFP expression in embryonic germinal zones

Brains from E14 to E19 NG2creBAC:Z/EG double tg embryos were examined to determine whether NG2 or EGFP was expressed by radial glia or by immature cells of the germinal zones of the ventricular zone (VZ) and SVZ. We did not detect NG2 or EGFP expression in GLAST+ radial glial cells throughout the forebrain. Fig. 7C,D shows images from the ventral tip of the posterior horn of the lateral ventricle at E18. The radial glial cells lining the VZ, whose cell bodies were labeled with DAPI (Fig. 7D), did not express NG2 or EGFP. EGFP and NG2 expression was confined to the vasculature in the VZ and SVZ. Further ventrally, ventral to the SVZ, there was a region in the ventral parenchyma where all the EGFP+ cells expressed NG2 and were either vascular cells or parenchymal cells with the typical appearance of NG2 glia with long slender processes (Fig. 7E). Further ventral to this EGFP+NG2+ glial zone was the region described above in which clusters of EGFP+NG2+ cells and EGFP+GLAST+ cells were found intermingled with each other. The presence of a zone consisting purely of EGFP+NG2+ cells and free of EGFP+ astrocytes between the ventral VZ/SVZ and the cluster of EGFP+ astrocytes near the ventral pial surface (Fig. 7F) suggests that it is unlikely that EGFP+ astrocytes were derived from EGFP+ cells in the germinal zones. Instead they are likely to have been generated from EGFP+NG2+ cells locally in the ventral parenchyma. The absence of NG2+ or EGFP+ cells in the SVZ might explain our failure to detect a significant number of reporter-positive neurons in the olfactory bulb (X.Z., M. Komitova and A.N., unpublished; M. Komitova and A.N., unpublished).

DISCUSSION
NG2 cell-specific expression of transgenes in NG2BAC tg mice

We have generated transgenic mouse lines, NG2DsRedBAC and NG2creBAC, in which the transgene is expressed specifically in NG2 cells at a high level. These NG2BAC tg mice represent the first transgenic mice that express transgenes specifically in NG2 and not in mature oligodendrocytes (Wight et al., 1993; Mallon et al., 2002; Gravel et al., 1998; Yuan et al., 2002). We have now generated several BAC tg mouse lines that express different genes using the same BAC building vector. Although the level of tg expression varies from line to line, the tissue specificity of tg expression in vivo is highly reproduced in the different lines (R. Suzuki and A.N., unpublished observations). The high degree of reproducibility of NG2 cell-specific pattern of expression using the NG2 BAC building vector described here makes this a powerful method for targeting various genes to NG2 cells.

Fate of NG2+DsRed+ cells in culture

The NG2DsRedBAC tg mice have enabled us to directly and exclusively select for NG2 cells by FACS to study their fate potential. The sorting gate was set stringently to ensure that 100%
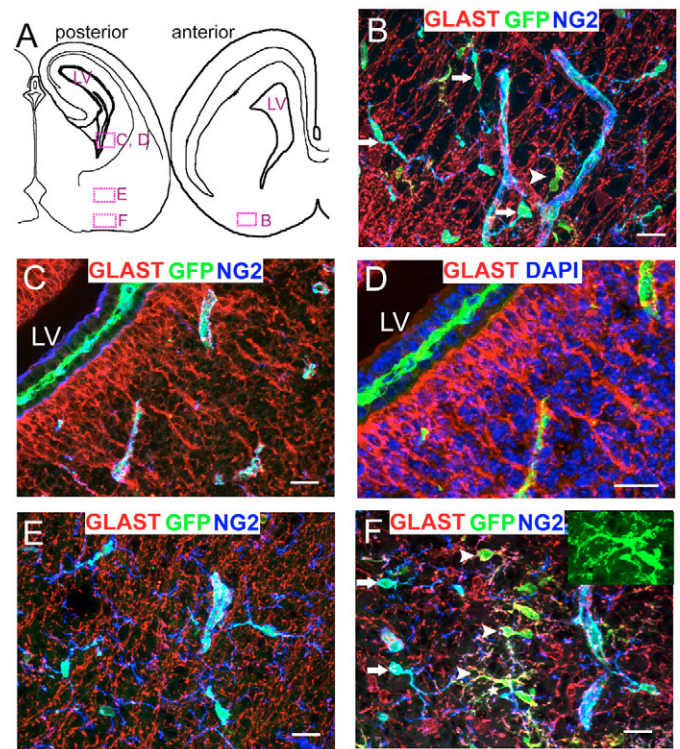

Fig. 7. Distribution of EGFP+ cells in embryonic forebrain of NG2creBAC:Z/EG double tg mice. Coronal sections (20 μm) through the forebrain of an E18 double tg mouse were triple labeled with mouse anti-GFP (green in B,C,E,F), rabbit anti-NG2 (blue in B,C,E,F), and rabbit anti-GLAST (red in B,C,D,E,F) antibodies. Dorsal is top, medial is left in B and right in C-F. (**A**) The drawings represent E18 posterior (left) and anterior (right) forebrains. The boxed areas indicate locations of the images in B-F. LV, lateral ventricle. (**B**) A coronal section through the ventral subpial region of anterior forebrain. Pial surface is lower left. The majority of EGFP+ cells in anterior ventral forebrain express NG2 (arrows). A small number of EGFP+ cells express GLAST and are NG2– (arrowhead). (**C**) Ventral ventricular zone of posterior forebrain showing the ventral tip of the posterior horn of the lateral ventricle. EGFP is not expressed in GLAST+ radial glia extending from the ventral germinal zone. EGFP and NG2 expression in the SVZ is restricted to vascular cells. (**D**) A higher magnification of the image shown in C stained for GLAST and DAPI. The cells bodies of radial glia in the ventricular zone are labeled by GLAST and are negative for GFP. Strong EGFP expression seen in the lateral ventricle in C and D is in the choroid plexus. (**E**) A region immediately ventral to the ventral tip of the SVZ underlying the ventral VZ. All the EGFP+ cells in this region express NG2. GLAST+ radial glial fibers are EGFP-negative. EGFP+NG2+ cells in the parenchyma have long slender processes. (**F**) A region ventral to E, adjacent to the ventral pial surface. Clusters of EGFP+ cells localized close to the ventral pial surface consist of two cell types: EGFP+NG2+ cells with long slender processes (arrows) and EGFP+GLAST+ cells (arrowheads) with little or no NG2. Some of the latter EGFP+GLAST+ cells have bushy processes resembling immature protoplasmic astrocytes (cell with a star, shown in green channel in inset). Scale bars: 20 μm.

of the sorted cells were DsRed+, which resulted in exclusion of some cells with low DsRed fluorescence. Under these conditions, an average of 3.3% of the total cells from the cerebral cortex, subcortical white matter and SVZ were sorted. NG2+ cells constituted more than 98% of the sorted cells, whereas O1+ oligodendrocytes accounted for 1-5%. Cells that did not express

NG2 are likely to be cells that had differentiated into O1+ cells during the 5 hours between the time of sorting and staining, or cells that had downregulated NG2 but still expressed DsRed due to the longer half-life of the latter.

The majority of the sorted cells remained as NG2+ cells, and fewer than 20% of the cells became oligodendrocytes. This is similar to the in vivo situation where NG2 glia persist in large numbers in the mature brain and are not depleted after oligodendrocyte differentiation. Cells that have *cnp* promoter activity and express NG2 were shown to differentiate into neurons (Belachew et al., 2003; Aguirre et al., 2004; Aguirre and Gallo, 2004; Roy et al., 1999; Nunes et al., 2003). In our study, we did not observe neuronal differentiation from sorted DsRed+ cells under conditions that had caused neuronal differentiation of SVZ cells. The discrepancy may be attributed to differences in the sorted cell population. The present study was conducted with cells that robustly expressed DsRed and NG2 and excluded cells with weak or marginal expression of NG2.

In addition to oligodendrocyte lineage cells, GFAP+ cells emerged from purified DsRed+ cells. They consisted not only of stellate type-2 astrocyte-like cells first described by Raff and colleagues (Raff et al., 1983) but also of flat pancake-shaped cells described by Miller and Szigeti (Miller and Szigeti, 1991). All the GFAP+ cells that appeared in cultures of sorted DsRed+ cells expressed NG2 at 4 div and were detected in all six independent cultures of sorted cells, which makes it unlikely that GFAP+ cells arose from contaminating cells that were initially NG2–. Nor is it likely that NG2+GFAP+ cells were caused by transgenic manipulation, since GFAP+NG2+ cells were also observed in secondary glial cultures obtained from P3 wt mouse and rat brains by the shaking method (McCarthy and de Vellis, 1980; Yang et al., 2005), and many of them expressed A2B5, although the proportion of NG2+ cells that expressed A2B5 was greater in rat cells. The appearance of some GFAP+ cells that were NG2-negative after 11 div suggests that GFAP+NG2+ cells give rise to GFAP+NG2– cells.

Fate of NG2+Cre+ cells in vivo

We used NG2creBAC tg mice crossed to Z/EG reporter mice (Novak et al., 2000) to examine whether NG2 glia give rise to astrocytes in vivo. Cre immunoreactivity was detected exclusively in NG2 cells. Not all NG2+ cells contained immunohistochemically detectable levels of Cre. This may be due to a low level of Cre in these cells below the threshold of antibody detection, or the absence of *cre* transcription in a small subpopulation of NG2+ cells. In NG2creBAC:Z/EG double tg mice, more than 85% of NG2+ cells were EGFP+. NG2+ cells that were EGFP-negative could represent NG2+ cells that failed to express Cre and/or incomplete target excision in Cre-expressing cells.

NG2+Cre+ cells generate myelinating oligodendrocytes

In NG2creBAC:Z/EG double tg mice, EGFP was detected in 78% of oligodendrocytes and myelin in the corpus callosum and striatal white matter at P14 and later time points. EGFP+ oligodendrocytes with myelinating processes were also found in the neocortex, indicating that NG2 glia generate myelinating oligodendrocytes in both white and gray matter. These observations provide direct evidence for the first time that endogenous NG2 glia give rise to myelinating oligodendrocytes in both gray and white matter. The presence of some oligodendrocytes that did not express EGFP may reflect incomplete Cre-mediated excision in NG2 glia and/or heterogeneity of reporter expression among oligodendrocytes.

Although it is less likely, the existence of other sources of oligodendrocytes besides NG2-positive precursors cannot be ruled out.

NG2+Cre+ cells generate protoplasmic but not fibrous astrocytes

In addition to oligodendrocytes, we observed in NG2creBAC:Z/EG double tg mice numerous EGFP+NG2– cells with highly branched, fine, bushy processes resembling protoplasmic astrocytes (Bushong et al., 2002). These EGFP+ astrocytes were most prevalent in the gray matter of the ventral posterior forebrain, where they constituted nearly half of S100β+ astrocytes, and some contained GFAP. Very few EGFP+ astrocytes were found in the dorsal cortex. Interestingly, there were no EGFP+ astrocytes in white matter. The observed regional difference in the prevalence of EGFP+ astrocytes was not due to regional variation in the expression of the reporter EGFP in the Z/EG mice, since β-galactosidase, which is expressed in Z/EG mice prior to Cre-mediated excision, was detected in dorsal as well as ventral cortical regions and in white matter. Furthermore, a similar ventral distribution of Cre reporter expression was observed when NG2creBAC mice were crossed to the ROSA26R reporter line (Soriano, 1999). Curiously, there seems to be a reciprocal distribution of EGFP+ astrocytes and oligodendrocytes derived from Emx1-expressing cortical progenitor cells (Kessaris et al., 2006). The astrogliogenic potential of NG2 glia may depend on their site of origin. Alternatively, environmental factors in the dorsal forebrain may be restricting the manifestation of their astrogliogenic fate.

The presence of cells that appeared to be in transition from NG2 glia to NG2– protoplasmic astrocytes provide additional support that NG2 glia differentiate into protoplasmic astrocytes. These intermediate EGFP+ cells were found as early as E18 and could be detected through P14 in NG2creBAC:Z/EG double tg mice. They had faint NG2 immunoreactivity restricted to the distal portions of their processes and had thicker proximal processes than the typical NG2 glia. These faintly NG2+ astrocyte-like cells had broadened web-like end-feet on blood vessels, a feature that is rarely seen in postnatal NG2 glia. These vascular contacts of the intermediate cells resembled those described for immature astrocytes by Zerlin and Goldman (Zerlin and Goldman, 1997). EGFP+ astrocytes increased in number in NG2creBAC:Z/EG double tg mice between E18 and P14 and persisted through P60. They were often seen in clusters, suggesting local proliferation of either newly generated astrocytes or NG2+ precursors. The presence of clusters of EGFP+ astrocytes in close proximity to EGFP+ myelinating oligodendrocytes seems to suggest that both oligodendrocytes and protoplasmic astrocytes can be generated from single NG2 cells, but clonal analysis in vivo is needed to confirm this. Further studies using inducible Cre in NG2 cells are currently under way to examine the timing of generation of astrocytes from NG2 cells.

Radial glia and SVZ progenitors are known to generate telencephalic astrocytes (Voigt, 1989; Levison and Goldman, 1993; Parnavelas, 1999), but the origin of astrocytes in different forebrain regions is not clear. Since neither NG2 nor EGFP was detected in radial cells or SVZ cells in the embryonic forebrain of NG2creBAC:Z/EG double tg mice, it is unlikely that transient activation of Cre in these early immature cells had caused reporter expression in astrocytes. The clustered distribution of EGFP+ astrocytes near the ventral pial surface at E18 is more indicative of a local differentiation from parenchymal NG2+ cells into protoplasmic gray matter astrocytes. This is further supported by the presence of a zone of EGFP+NG2+ cells lacking EGFP+ astrocytes that separated the ventral VZ/SVZ from the ventral subpial cluster

of EGFP+ astrocytes (Fig. 7F), making it unlikely that EGFP+ astrocytes had been generated from Cre+ or GFP+ cells in the SVZ. Perhaps radial glia and SVZ progenitor cells generate astrocytes in white matter and dorsal neocortex, whereas NG2 glia give rise to astrocytes in ventral forebrain.

Transplanted OPCs have not been shown to generate astrocytes in the host CNS (Groves et al., 1993; Espinosa de los Monteros et al., 1993) except under pathological astrocyte-free conditions (Franklin et al., 1995). Based on these observations, the astrocytic fate of OPCs [O-2A progenitor cells (Raff et al., 1983)] has been generally discarded as an in vitro artifact. However, since transplanted cells preferentially migrate along white matter tracts, it is possible that these studies had examined the fate of OPCs in regions where the environment does not support astrocyte differentiation from these cells. Further studies are needed to elucidate whether NG2 cell-derived astrocytes are functionally distinct from other astrocytes that exist in the brain.

Supplementary material
Supplementary material for this article is available at
http://dev.biologists.org/cgi/content/full/135/1/145/DC1

References
Aguirre, A. and Gallo, V. (2004). Postnatal neurogenesis and gliogenesis in the olfactory bulb from NG2-expressing progenitors of the subventricular zone. *J. Neurosci.* **24**, 10530-10541.
Aguirre, A. A., Chittajallu, R., Belachew, S. and Gallo, V. (2004). NG2-expressing cells in the subventricular zone are type C-like cells and contribute to interneuron generation in the postnatal hippocampus. *J. Cell Biol.* **165**, 575-589.
Belachew, S., Chittajallu, R., Aguirre, A. A., Yuan, X., Kirby, M., Anderson, S. and Gallo, V. (2003). Postnatal NG2 proteoglycan-expressing progenitor cells are intrinsically multipotent and generate functional neurons. *J. Cell Biol.* **161**, 169-186.
Bevis, B. J. and Glick, B. S. (2002). Rapidly maturing variants of the Discosoma red fluorescent protein (DsRed). *Nat. Biotechnol.* **20**, 83-87.
Bhat, R. V., Axt, K. J., Fosnaugh, J. S., Smith, K. J., Johnson, K. A., Hill, D. E., Kinzler, K. W. and Baraban, J. M. (1996). Expression of the APC tumor suppressor protein in oligodendroglia. *Glia* **17**, 169-174.
Bu, J., Akhtar, N. and Nishiyama, A. (2001). Transient expression of the NG2 proteoglycan by a subpopulation of activated macrophages in an excitotoxic hippocampal lesion. *Glia* **34**, 296-310.
Bu, J., Banki, A., Wu, Q. and Nishiyama, A. (2004). Increased NG2(+) glial cell proliferation and oligodendrocyte generation in the hypomyelinating mutant shiverer. *Glia* **48**, 51-63.
Bushong, E. A., Martone, M. E., Jones, Y. Z. and Ellisman, M. H. (2002). Protoplasmic astrocytes in CA1 stratum radiatum occupy separate anatomical domains. *J. Neurosci.* **22**, 183-192.
Dawson, M. R., Levine, J. M. and Reynolds, R. (2000). NG2-expressing cells in the central nervous system: are they oligodendroglial progenitors? *J. Neurosci. Res.* **61**, 471-479.
Dawson, M. R., Polito, A., Levine, J. M. and Reynolds, R. (2003). NG2-expressing glial progenitor cells: an abundant and widespread population of cycling cells in the adult rat CNS. *Mol. Cell. Neurosci.* **24**, 476-488.
Espinosa de los Monteros, A., Zhang, M. and de Vellis, J. (1993). O2A progenitor cells transplanted into the neonatal rat brain develop into oligodendrocytes but not astrocytes. *Proc. Natl. Acad. Sci. USA* **90**, 50-54.
Franklin, R. J. M., Bayley, S. A., Milner, R., ffrench-Constant, C. and Blakemore, W. F. (1995). Differentiation of the O-2A progenitor cell line CG-4 into oligodendrocytes and astrocytes following transplantation into glia-deficient areas of CNS white matter. *Glia* **13**, 39-44.
Gravel, M., Di Polo, A., Valera, P. B. and Braun, P. E. (1998). Four-kilobase sequence of the mouse CNP gene directs spatial and temporal expression of lacZ in transgenic mice. *J. Neurosci. Res.* **53**, 393-404.
Groves, A. K., Barnett, S. C., Franklin, R. J. M., Crang, A. J., Mayer, M., Blakemore, W. F. and Noble, M. (1993). Repair of demyelinated lesions by transplantation of purified O-2A progenitor cells. *Nature* **362**, 453-455.
Heintz, N. (2001). BAC to the future: the use of bac transgenic mice for neuroscience research. *Nat. Rev. Neurosci.* **2**, 861-870.
Horner, P. J., Power, A. E., Kempermann, G., Kuhn, H. G., Palmer, T. D., Winkler, J., Thal, L. J. and Gage, F. H. (2000). Proliferation and differentiation of progenitor cells throughout the intact adult rat spinal cord. *J. Neurosci.* **20**, 2218-2228.
Kessaris, N., Fogarty, M., Iannarelli, P., Grist, M., Wegner, M. and Richardson, W. D. (2006). Competing waves of oligodendrocytes in the forebrain and postnatal elimination of an embryonic lineage. *Nat. Neurosci.* **9**, 173-179.
Levine, J. M., Stincone, F. and Lee, Y. S. (1993). Development and differentiation of glial precursor cells in the rat cerebellum. *Glia* **7**, 307-321.
Levison, S. W. and Goldman, J. E. (1993). Both oligodendrocytes and astrocytes develop from progenitors in the subventricular zone of postnatal rat forebrain. *Neuron* **10**, 201-212.
Mallon, B. S., Shick, H. E., Kidd, G. J. and Macklin, W. B. (2002). Proteolipid promoter activity distinguishes two populations of NG2-positive cells throughout neonatal cortical development. *J. Neurosci.* **22**, 876-885.
Matz, M. V., Fradkov, A. F., Labas, Y. A., Savitsky, A. P., Zaraisky, A. G., Markelov, M. L. and Lukyanov, S. A. (1999). Fluorescent proteins from nonbioluminescent Anthozoa species. *Nat. Biotechnol.* **17**, 969-973.
McCarthy, K. D. and de Vellis, J. (1980). Preparation of separate astroglial and oligodendroglial cell cultures from rat cerebral tissue. *J. Cell Biol.* **85**, 890-902.
McLean, I. W. and Nakane, P. K. (1974). Periodate-lysine-paraformaldehyde fixative. A new fixation for immunoelectron microscopy. *J. Histochem. Cytochem.* **22**, 1077-1083.
McTigue, D. M., Wei, P. and Stokes, B. T. (2001). Proliferation of NG2-positive cells and altered oligodendrocyte numbers in the contused rat spinal cord. *J. Neurosci.* **21**, 3392-3400.
Miller, R. H. and Szigeti, V. (1991). Clonal analysis of astrocyte diversity in neonatal rat spinal cord cultures. *Development* **113**, 353-362.
Nishiyama, A., Lin, X.-H., Giese, N., Heldin, C.-H. and Stallcup, W. B. (1996a). Co-localization of NG2 proteoglycan and PDGF α receptor on O2A progenitor cells in the developing rat brain. *J. Neurosci. Res.* **43**, 299-314.
Nishiyama, A., Lin, X.-H., Giese, N., Heldin, C.-H. and Stallcup, W. B. (1996b). Interaction between NG2 proteoglycan and PDGF α receptor on O2A progenitor cells is required for optimal response to PDGF. *J. Neurosci. Res.* **43**, 315-330.
Nishiyama, A., Watanabe, M., Yang, Z. and Bu, J. (2002). Identity, distribution, and development of polydendrocytes: NG2-expressing glial cells. *J. Neurocytol.* **31**, 437-455.
Nishiyama, A., Yang, Z. and Butt, A. (2005). Astrocytes and NG2-glia: what's in a name? *J. Anat.* **207**, 687-693.
Novak, A., Guo, C., Yang, W., Nagy, A. and Lobe, C. G. (2000). Z/EG, a double reporter mouse line that expresses enhanced green fluorescent protein upon Cre-mediated excision. *Genesis* **28**, 147-155.
Nunes, M. C., Roy, N. S., Keyoung, H. M., Goodman, R. R., McKhann, G., 2nd, Jiang, L., Kang, J., Nedergaard, M. and Goldman, S. A. (2003). Identification and isolation of multipotential neural progenitor cells from the subcortical white matter of the adult human brain. *Nat. Med.* **9**, 439-447.
Ozerdem, U., Grako, K. A., Dahlin-Huppe, K., Monosov, E. and Stallcup, W. B. (2001). NG2 proteoglycan is expressed exclusively by mural cells during vascular morphogenesis. *Dev. Dyn.* **222**, 218-227.
Parnavelas, J. G. (1999). Glial cell lineages in the rat cerebral cortex. *Exp. Neurol.* **156**, 418-429.
Peters, A. (2004). A fourth type of neuroglial cell in the adult central nervous system. *J. Neurocytol.* **33**, 345-357.
Polito, A. and Reynolds, R. (2005). NG2-expressing cells as oligodendrocyte progenitors in the normal and demyelinated adult central nervous system. *J. Anat.* **207**, 707-716.
Pringle, N. P., Mudhar, H. S., Collarini, E. J. and Richardson, W. D. (1992). PDGF receptors in the rat CNS: during late neurogenesis, PDGF alpha-receptor expression appears to be restricted to glial cells of the oligodendrocyte lineage. *Development* **115**, 535-551.
Raff, M. C., Miller, R. H. and Noble, M. (1983). A glial progenitor cell that develops in vitro into an astrocyte or an oligodendrocyte depending on culture medium. *Nature* **303**, 390-396.
Rao, M. S. and Mayer-Proschel, M. (1997). Glial-restricted precursors are derived from multipotent neuroepithelial stem cells. *Dev. Biol.* **188**, 48-63.
Reynolds, R. and Hardy, R. (1997). Oligodendroglial progenitors labeled with the O4 antibody persist in the adult rat cerebral cortex in vivo. *J. Neurosci. Res.* **47**, 455-470.
Reynolds, R., Dawson, M., Papadopoulos, D., Polito, A., Di Bello, I. C.,

Pham-Dinh, D. and Levine, J. (2002). The response of NG2-expressing oligodendrocyte progenitors to demyelination in MOG-EAE and MS. *J. Neurocytol.* **31**, 523-536.

Roy, N. S., Wang, S., Harrison-Restelli, C., Benraiss, A., Fraser, R. A., Gravel, M., Braun, P. E. and Goldman, S. A. (1999). Identification, isolation, and promoter-defined separation of mitotic oligodendrocyte progenitor cells from the adult human subcortical white matter. *J. Neurosci.* **19**, 9986-9995.

Soriano, P. (1999). Generalized lacZ expression with the ROSA26 Cre reporter strain. *Nat. Genet.* **21**, 70-71.

Trapp, B. D., Nishiyama, A., Cheng, D. and Macklin, W. B. (1997). Differentiation and death of premyelinating oligodendrocytes in developing rodent brain. *J. Cell Biol.* **137**, 459-468.

Vecchi, A., Garlanda, C., Lampugnani, M. G., Resnati, M., Matteucci, C., Stoppacciaro, A., Schnurch, H., Risau, W., Ruco, L., Mantovani, A. et al. (1994). Monoclonal antibodies specific for endothelial cells of mouse blood vessels. Their application in the identification of adult and embryonic endothelium. *Eur. J. Cell Biol.* **63**, 247-254.

Verity, A. N., Bredesen, D., Vonderscher, C., Handley, V. W. and Campagnoni, A. T. (1993). Expression of myelin protein genes and other myelin components in an oligodendrocytic cell line conditionally immortalized with a temperature-sensitive retrovirus. *J. Neurochem.* **60**, 577-587.

Voigt, T. (1989). Development of glial cells in the cerebral wall of ferrets: direct tracing of their transformation from radial glia into astrocytes. *J. Comp. Neurol.* **289**, 74-88.

Watanabe, M., Toyama, Y. and Nishiyama, A. (2002). Differentiation of proliferated NG2-positive glial progenitor cells in a remyelinating lesion. *J. Neurosci. Res.* **69**, 826-836.

Wight, P. A., Duchala, C. S., Readhead, C. and Macklin, W. B. (1993). A myelin proteolipid protein-LacZ fusion protein is developmentally regulated and targeted to the myelin membrane in transgenic mice. *J. Cell Biol.* **123**, 443-454.

Yang, X. W., Model, P. and Heintz, N. (1997). Homologous recombination based modification in Escherichia coli and germline transmission in transgenic mice of a bacterial artificial chromosome. *Nat. Biotechnol.* **15**, 859-865.

Yang, Z., Watanabe, M. and Nishiyama, A. (2005). Optimization of oligodendrocyte progenitor cell culture method for enhanced survival. *J. Neurosci. Methods* **149**, 50-56.

Yarbrough, D., Wachter, R. M., Kallio, K., Matz, M. V. and Remington, S. J. (2001). Refined crystal structure of DsRed, a red fluorescent protein from coral, at 2.0-A resolution. *Proc. Natl. Acad. Sci. USA* **98**, 462-467.

Yuan, X., Chittajallu, R., Belachew, S., Anderson, S., McBain, C. J. and Gallo, V. (2002). Expression of the green fluorescent protein in the oligodendrocyte lineage: a transgenic mouse for developmental and physiological studies. *J. Neurosci. Res.* **70**, 529-545.

Zerlin, M. and Goldman, J. E. (1997). Interactions between glial progenitors and blood vessels during early postnatal corticogenesis: blood vessel contact represents an early stage of astrocyte differentiation. *J. Comp. Neurol.* **387**, 537-546.